DOVER MOTION
A division of Invetech

159 Swanson Rd.
Boxborough, MA 01719
Phone +1.508.475.3400
dovermotion.com

A Constant Velocity Scanning Stage with a Resolution of 31 Picometers

By Kevin J. McCarthy, Chief Technology Officer

Abstract: This paper describes a constant velocity scanning stage with a resolution of 31 picometers. For comparison purposes, the classical Bohr radius of the hydrogen atom is 53 picometers. The primary structural element of the stage is a precision lapped granite beam. The moving carriage is guided over a travel of 270 mm by a two-sided air bearing, incorporating porous stainless steel flow restrictors and magnetic preload. Drive is provided by a single-sided, ironless, three-phase moving magnet linear motor, with phase currents sourced by a proprietary linear amplifier. A commercial motion controller closes the position and velocity loops, with a servo bandwidth of 75 Hz. Position feedback is provided by a linear optical encoder, with a grating pitch of 512 nanometers, and an electrical period of 128 nanometers. The analog quadrature signals are acquired by a pair of high-speed 14 bit A:D converters, and the arc-tan conversion results in a final resolution of 31 picometers. A homodyne laser interferometer also monitors the stage position, with a resolution of 77 picometers. FFT analysis of the position tracking error reveals a cyclical error component in the laser interferometer. With this error subtracted, the tracking error during constant velocity motion is approximately 1 nanometer at a scan velocity of 10 micrometers per second.

While the pace of product development has cooled significantly from the brief but heady days of the photonics boom, dense wave division multiplexing (DWDM) continues to challenge the state of the art in precision positioning systems. One particularly exacting application lies in the production of fiber Bragg gratings (FBGs). An FBG is a very narrow band (< 1 Angstrom FWFZ), high-reflectance mirror formed within a specially doped optical fiber, which efficiently transmits wavelengths above or below the Bragg mirror wavelength. Bragg reflection within the photosensitized fiber is achieved by using a UV laser light source, first order diffraction with a phase grating, and constant velocity scanning motion to induce a permanent, periodic variation in the fiber's refractive index. These periodic index variations function for infrared light in exactly the same manner as X-rays experience Bragg reflection off successive atomic planes within a crystal lattice. The typical spatial period of these induced index variations is ~ 0.5 microns (for the preferred 1550 nm. telecom wavelength band), and very tight control of the UV dose leads to correspondingly strict tolerances on the scanning velocity. In addition, direct FBG writing requires a high degree of stage accuracy if the resulting grating is to maintain phase coherence over its length. Additional goals such as side-lobe suppression via grating apodization, and non-uniform period "chirped" gratings to compensate for chromatic dispersion, place further demands upon the positioning system. These various and stringent requirements led us to

design a positioning stage, dubbed the “Bragg-o-matic”, which would provide the highest available levels of precision in point-to-point, constant velocity, and modulated velocity motion.

The application requirements could best be met with a single axis, linear positioning stage, whose travel was dictated by the longest grating to be written - a bit over 240 mm, along with some provision for overtravel. We sought to design a stage that would as nearly as possible approximate an idealized “physics package”, with minimal corrupting influences. This led us to choose air bearings for the linear guideways, which are nearly friction free, and very effectively constrain motion to a single degree of freedom. A photo of the stage is shown in Fig.1

Fig 1: Air bearings and Linear guideways stage

The base structure that the air bearing carriage floats upon is a precision lapped beam of high modulus granite. This material offers high dimensional stability, a low coefficient of thermal expansion (~ 5 ppm/deg. C), and can be easily lapped to high precision. The granite base is supported on three locking, fine-pitch, adjustable mounting feet. The lightweighted steel air bearing carriage is of a “two-sided” design, with magnetic preload. Permanent magnets and isolated flux directing elements within the carriage provide an attractive force in two axes against preload strips embedded in the granite base spar. To eliminate hysteretic drag and direction dependent angular errors, these preload strips are fabricated from a nickel-steel alloy with very low hysteretic losses. Identical preload strips were installed in the two opposing faces of the granite spar to prevent angular errors due to their differential thermal coefficient of expansion. The discrete air bearing restriction elements within the carriage plates are fabricated using porous stainless steel; these are nearly clog-free, and their low air exit velocity significantly reduces position tracking errors due to granite surface microstructure. Air bearing gaps were maintained at 7 microns.

The use of mechanical drive methods was ruled out due to their intrinsically influencing nature, non-zero and fluctuating friction, and cyclical errors. We accordingly chose a direct drive linear motor, for which several motor topologies were available. Single phase linear motors scale rather badly as the travel is increased, with magnetic saturation leading to quite bulky motor assemblies. While the commutation of multi-phase linear motors can be a low-level source of positioning errors, the quite low velocities associated with this application (1 to

1000 um/sec) would benefit from very large amounts of integrator gain at the commutation frequency. We also sought to eliminate any perturbations due to moving cables. Our final selection for the linear motor was a custom three phase, moving magnet design, with a stationary coil assembly centered on the upper face of the granite base spar, and a single-sided, periodic array of permanent magnets pole pairs mounted to the underside of the moving carriage. This design has the benefit that the motor cables are stationary; while the moving carriage must grow as travel is increased, the resulting carriage length for this 270 mm. travel application was close to that required for the customer's fixturing. The steel carriage plate immediately behind the permanent magnet array improves the gap flux and hence the motor Km, but the absence of ferrous materials in the coil assembly eliminates any potential for cogging.

Having selected a stiff, frictionless air bearing guideway, and a non-contact, direct drive, ironless linear motor, the remaining critical design choices are the position feedback device, and the drive/control system. These both play a role in determining the magnitude of position errors, with the feedback system contributing to both accuracy and uncertainty (jitter), while the control/drive system affects only uncertainty.

Modern control systems are invariably digital in nature, while amplifiers can nominally be either analog or digital. This distinction is somewhat misleading, as "digital" amplifiers derive their current information from an analog current sensor and an A:D converter, while "analog" amplifiers are commanded by a digital DAC. In both cases, there is a critical digital conversion whose quantization of the process leads to limit cycle oscillations. Current commercially available control/drive systems tend toward either digital PWM current control with 12 or 14 bit A:D converters, or analog amplifiers commanded by 12 to 18 bit DACs. For very high resolution systems, we prefer linear (analog) amplifiers to PWM (digital) solutions, as their digital quantization is finer, and they do not produce electrical noise that can couple into low-level signals. In either case, one can calculate the magnitude of the limit cycle oscillation produced by the inevitable digital conversion. For ± 10 volt input, DAC commanded analog amplifiers, this is:

$$\Delta X = \frac{K_{dac} \bullet K_{amp} \bullet K_f \bullet \tau^2}{2 \bullet M} \qquad \text{where } K_{dac} = \frac{10\ V}{2^{n-1}} \qquad \text{and } \tau = \frac{1}{2\ \pi\ f_0}$$

In the case of this stage, for which the DAC resolution n is 18 bits, the amplifier transconductance gain K_{amp} is 1.0 amp/volt, the motor force constant Kf is 4.6 Newtons per amp, the stage moving mass is 7.4 kg, and the servo bandwidth f0 is 75Hz, the resulting amplitude of the DAC-induced limit cycle oscillation is a tolerable 107 picometers. With more typical commercial DAC resolutions of 12 bits, this effect would have been far more pronounced, at ~7 nanometers

The motion controller used for this system was a Delta-Tau PMAC2-PCI. The scaling of the position and velocity loop filters on this controller can accommodate a very wide range of resolutions without difficulty, and its 18 bit DACs minimize the effect of DAC quantization. The position loop was closed at a sample rate of 5 kHz, which significantly reduced phase shift at the servo bandwidth due to the zero order hold. The amplifier chosen in this application is the Danaher Motion "NanoDrive", which is a very low noise, three-phase, 300 watt linear transconduc-tance amplifier. Commutation is performed within the Delta-Tau controller, and a pair of 18 bit DACs command the NanoDrive linear amplifier, performing a smooth and accurate sinusoidal commutation of the three motor phases.

Position uncertainty due to quantization is also present due to the finite resolution of the position feedback device, which must undergo a digital conversion at some point in its signal train. In this case, no calculation is necessary; the potential position jitter will simply equal the resolution of the position feedback device. The stage's moving carriage, suspended on its frictionless air bearing, is in effect inertially tied to the distant stars. Environmental acceleration moves the stage base relative to the carriage, and this differential movement must be large enough to exceed the position feedback device's digital resolution if the servo loop is to command a response. In essence, the feedback path has gone "open loop" for movements below the threshold of digital position feedback quantization. Mechanical stages behave a bit differently; while they lack true Coulomb friction, the local detent of their rolling element ways defines a mild potential well. The weak stiffness of this "well" provides more rejection of background acceleration than does a frictionless air bearing.

Two legitimate questions are "How much position feedback resolution is useful or needed, and can you have "too much""? To paraphrase the late Barry Goldwater: "Extreme resolution in the defense of precision is no vice". In general, more resolution is a good thing, and will reduce position uncertainty. More accurately, while arbitrarily increasing resolution has no negative impact other than cost, there finally comes a point beyond which further increases in resolution do not improve position jitter (Fig 2).

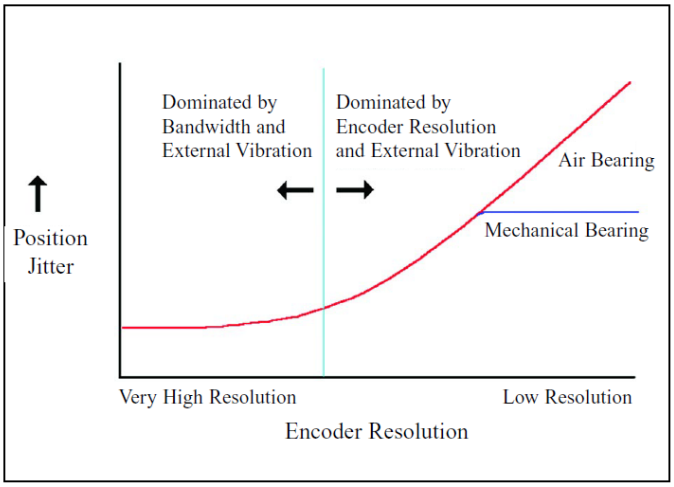

Fig. 2

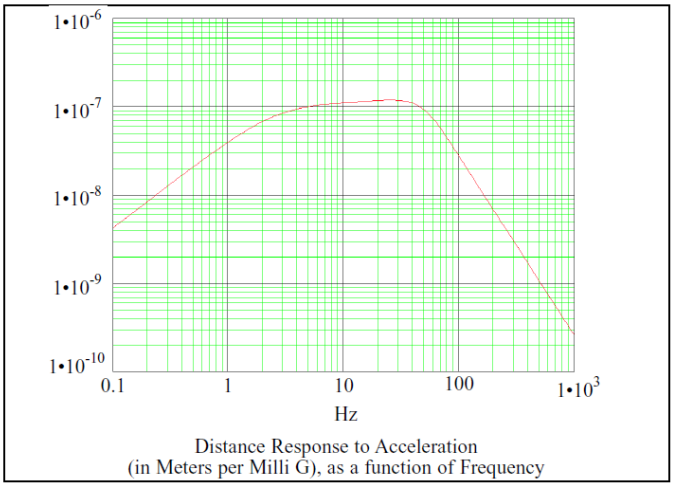

Fig. 3

At very coarse encoder resolutions, and in the presence of environmental acceleration, air bearing position jitter will equal the position feedback resolution, while for mechanical bearing stages, the jitter is capped by the local stiffness of the rolling element ways. As position feedback resolution is increased, jitter decreases, but eventually reaches a floor. This floor is due to the finite servo bandwidth, which presents a frequency dependent stiffness that attenuates, but does not eliminate, the effect of external accelerations. This is shown in Fig. 3, where the position response to acceleration, in meters per milli-G, is graphed as a function of frequency.

From DC to a few Hertz, the sensitivity to external acceleration rises linearly with frequency, with rejection of external disturbance provided by the position loop integrator. It is then roughly flat from there out to the servo bandwidth (75 Hz), due to the position loop proportional term, after which sensitivity falls off as the inverse square of frequency, due to the stage's mass. The conclusion to be reached from this analysis can be simply stated as "Use as much position resolution as you can afford, and then work hard on vibration isolation". Of course, as the effectiveness of the vibration isolation is increased, further demands can be justified for the position feedback resolution.

We ended up selecting a pair of position feedback devices: a linear optical encoder, and a laser interferometer. The linear encoder is a Heidenhain LIP 382, which is arguably the finest linear encoder in the world. It has a measuring length of 270 mm, and consists of a chrome-on-Zerodur phase grating, together with a read-head. The LIP 382 works via dual reflection, first order diffraction off the grating, whose physical pitch is 512 nanometers. The resulting electrical signal has a period of 128 nanometers, and is remarkably free of harmonics and cyclical error. Heidenhain's attempts to measure the cyclical error foundered in instrumental difficulties at ± 50 picometers. Overall accuracy for the full 270 mm measuring length is ± 50 nanometers. The 1 VPTP sine/cosine output of the encoder is routed to a pair of 14 bit A:D converters in the Delta-Tau interpolation card; this performs the arc-tan position calculation every servo sample, and implements a 4096X subdivision of the 128 nanometer signal period, for a nominal resolution of 31 picometers. The use of A:D based interpolation every servo cycle, as opposed to the more traditional real-time quadrature format, eliminates the trade-off of resolution vs. speed; this system maintains position fidelity at speeds to 200 mm/sec, despite its 31 picometer resolution. In our design, the read-head is stationary; this avoids the need for moving cables, and locates the read-head directly below the laser fiber writing position. While the LIP 382 is nearly perfect, it has one drawback – it cannot be physically located along the fiber axis, and hence will be subject to Abbe (offset) error. With air bearing guideway errors of ~ 10 microradians, the 90 mm physical offset of the encoder from the fiber axis results in an Abbe error of 0.90 microns, about an order of magnitude larger than the intrinsic errors of the encoder.

The laser interferometer is a Renishaw RLE-10, an innovative, high-performance, homodyne (single frequency) interferometer. It is fiber launched, which allows the laser head to be conveniently located away from the precision stage. The signal period is 316 nanometers in single-pass (retroreflector), and 158 nanometers in double-pass (plane mirror). For this application, we chose the simpler to align single-pass configuration, as the laser interferometer optical axis was designed to coincide with the fiber axis, and the retroreflector would need to be removed during operation and re-installed afterwards. The purpose of the laser interferometer was to measure the Abbe error at the fiber axis, and correct this via the use of compensation tables within the Delta-Tau controller. One distinct

advantage of using a homodyne laser interferometer is that its native output format is an analog 1 volt sine/cosine signal. As such, it can be easily interpolated to 4096X, using another channel of the Delta-Tau A:D based interpolator. The resulting resolution is 77 picometers, and error-free speeds to 500 mm/second at this resolution are possible (notwithstanding the fact that this is a very low speed application). Telescoping, non-contact tubes surround the beam to reduce air currents, and a gas fitting allows a helium purge of the beam path (the refractive index of helium is an order of magnitude lower than that of air, which can nearly eliminate errors due to refractive index variations). Multiple runs can be averaged, further enhancing Abbe errors over system noise. The fundamental accuracy of the laser interferometer is tied to its vacuum wavelength, which is in turn measured to high accuracy by beating it against an iodine reference laser.

With the accuracy inherent in the two feedback sources described above, most residual short-period errors are due to environmental vibration, while most long period errors are due to thermal effects. The use of low expansion granite for the base structure, to which both the encoder read-head and laser head are mounted, and the customer's provision of an Invar fiber mount and clamp, help reduce thermal effects. The facility in which it is installed also includes ± 0.5˚C temperature control, as well as conventional active-pneumatic vibration isolation. There are no moving cables in the design, but there is one small (3 mm diameter) compressed air line, which is suspended in a large radius tether during operation.

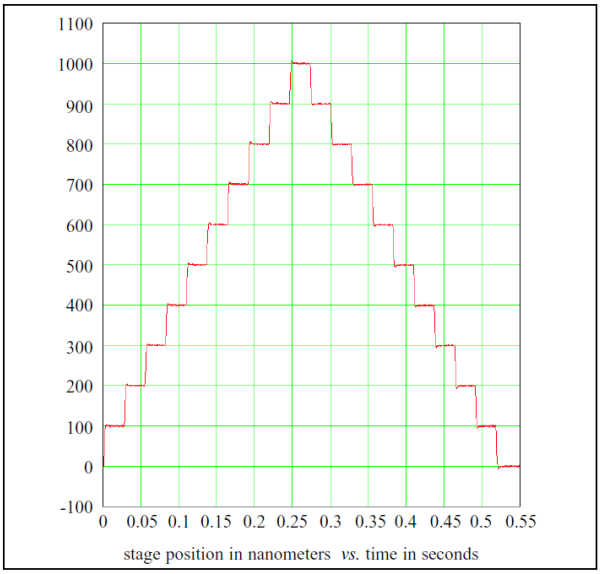

Fig. 4

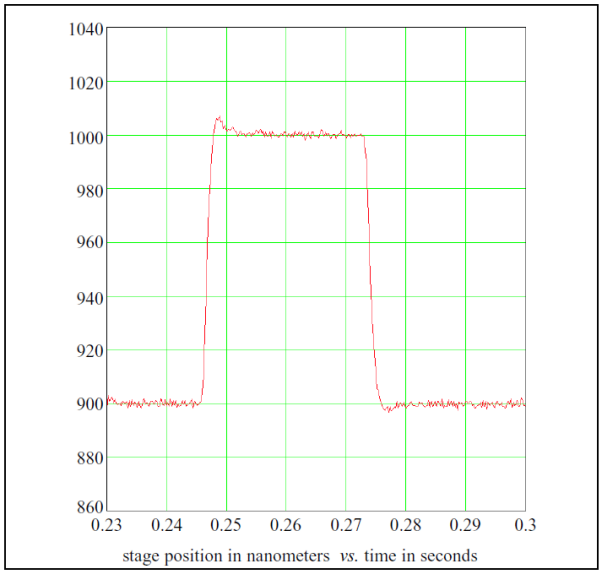

Fig. 5

The system tuned up to a conservative servo bandwidth of about 75 Hz, driven in part by a desire to gracefully accommodate any future plant payload mass changes. The ultimate limits to servo bandwidth were set by the first torsional resonance, due to the finite stiffness of the air bearings, together with controller latencies and the zero order hold due to the sample rate. Since this system will occasionally be operated in point-to-point mode, we acquired data for a position staircase (Fig. 4), including a zoom-in of the top step (Fig. 5). Position jitter during the staircase move had an amplitude of about ±1 nanometers.

Despite the very high accuracy of the LIP 382 linear encoder, examination of its position vs. time data while scanning would reveal little beyond external disturbances; the servo loop by definition attempts to drive position tracking error to zero. The last word in stage testing usually requires a separate laser interferometer measurement system. We began by setting up a Zygo ZMI-1000 in plane mirror mode, with a resolution of 1.24 nanometers. The first data sets on tracking error (deviation from nominal position during constant velocity motion) revealed quite good performance (Fig. 6), with tracking errors of ±3 nanometers at a scan velocity of 10 microns per second.

Position tracking error in nanometers *vs.* time in seconds

(Zygo ZMI-1000)

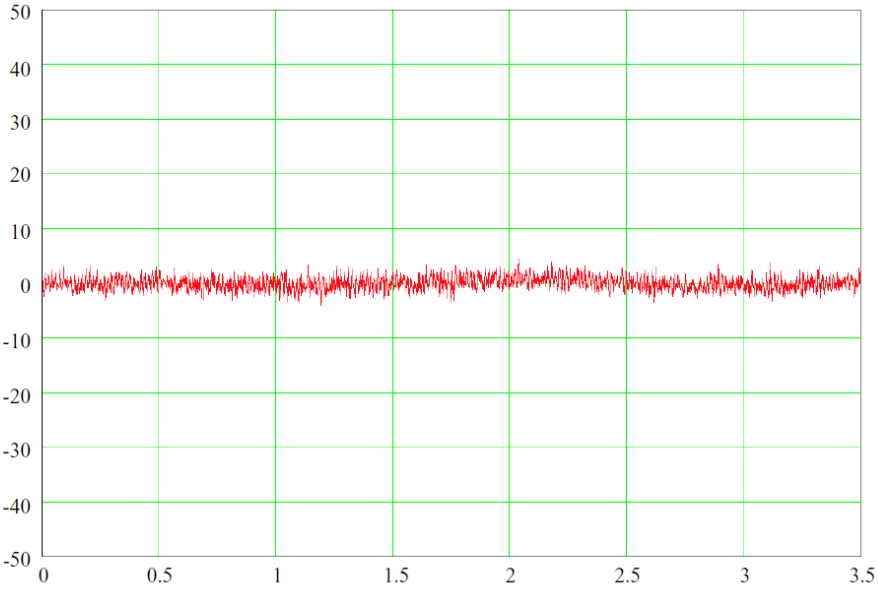

Fig. 6

A cursory examination of the position error vs. time data on a shorter time scale showed a distinctly sinusoidal component, so the natural next step was to perform an FFT on the data (Fig. 7) to determine its frequency.

FFT of position tracking error data nm. *vs.* Hz.

(Zygo ZMI-1000)

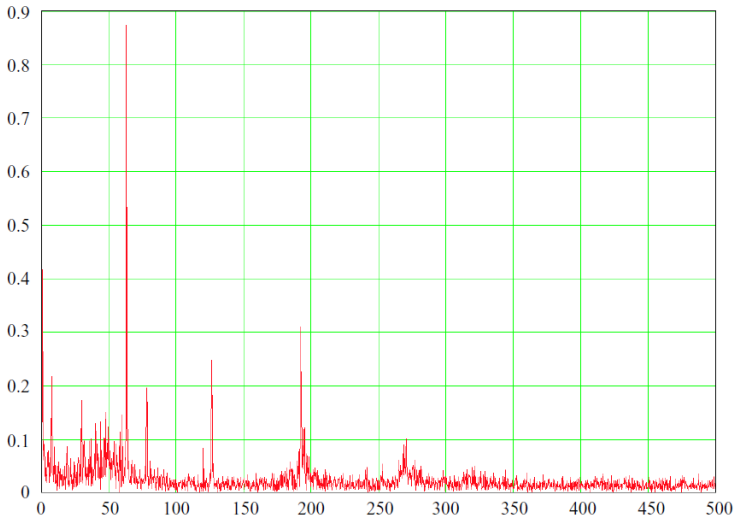

Fig. 7

We were dismayed to observe that bane of data collectors, a 60 Hz. component (with higher order harmonics), and concluded that we either had inadequate filtering on the amplifier power supply, or some line voltage electrical pick-up on the sinusoidal encoder inputs. The usual round of quick patches failed to attenuate these frequencies, and the suggestion that the noise was optically coupled from the room's fluorescent lights resulted in little other than our stumbling around in the dark. Once we found the light switch, we took a bit closer look at the FFT (Fig. 8):

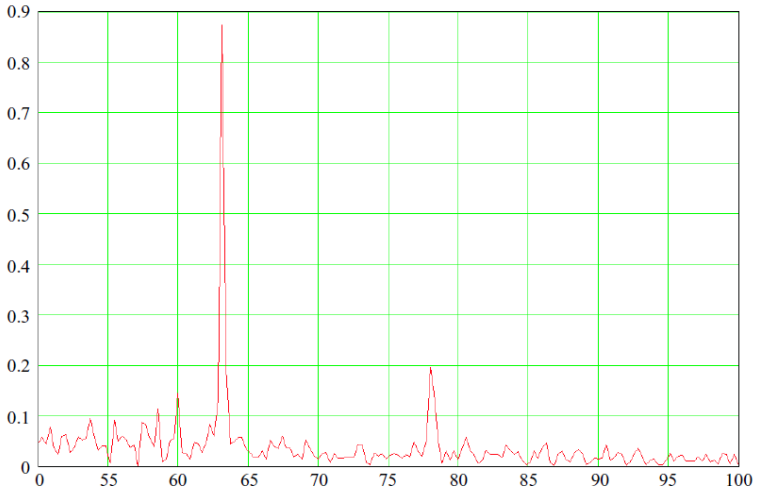

Fig. 8

The actual frequency of the dominant component was not exactly 60Hz, but 63.3 Hz... Hmmm... this number seemed oddly familiar. Converting this frequency to a spatial period told the tale: at 10 microns per second, the period of 158 nanometers happens to equal the plane mirror laser interferometer electrical period (one-quarter of the He-Ne 633 nm. wavelength). In a wry twist, the laser was able to measure its *own* cyclical error, by virtue of the fact that the actual stage motion was under the servo control of another position feedback device. The Heidenhain encoder has an electrical period of 128 nanometers, and this accounts for the small blip at 78 Hz, with an amplitude of 200 picometers. The 63.3, 126, and 190 Hz. cyclical error components are entirely an artifact of the measuring laser, and are probably tied to phase meter errors and/or polarization mixing. A quick speed change to 1 micron per second confirmed the hypothesis, and a look at the data from the Renishaw laser interferometer shows the expected result (Figures 9 and 10). While the physical mechanisms for cyclical error in the homodyne laser are no doubt different then that of the heterodyne, cyclical error was present and somewhat more pronounced, albeit with only the fundamental and first harmonic. These two frequency components shift down to 3.2 Hz. and 6.3 Hz. at this lower speed of 1 micron per second (recall that the Renishaw laser was operated in double-pass, with a 318 nanometer electrical period). With the laser interferometer cyclical error artifacts subtracted, and taking into account the inevitable presence of atmospheric refractive index fluctuations, the actual tracking errors of the stage during constant velocity motion are estimated to have an amplitude of ~1 nanometer.

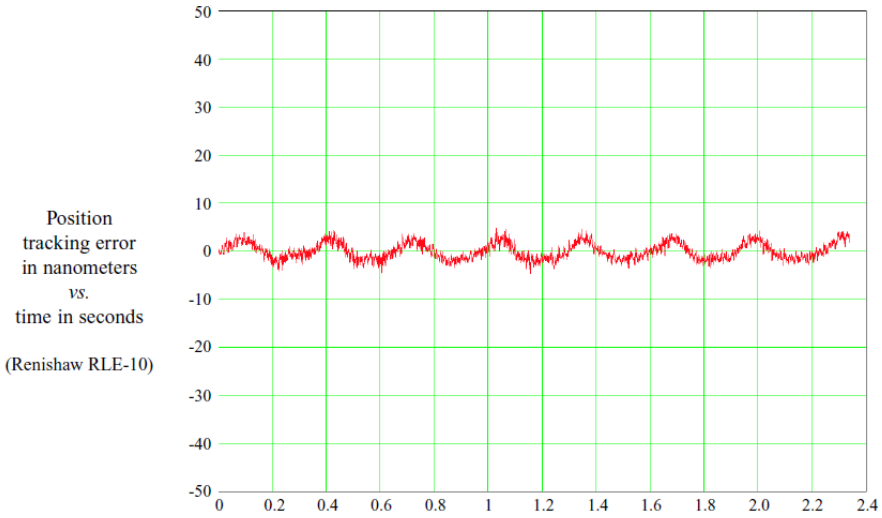

Fig. 9

FFT of Renishaw RLE-10 laser tracking error data nm. *vs.* Hz.

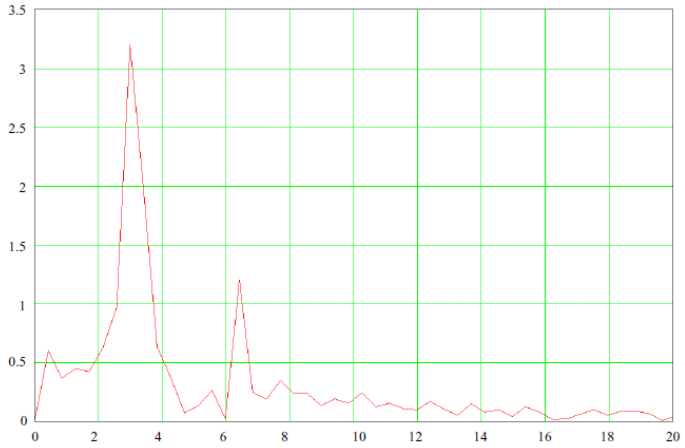

Fig. 10

All in all, both the customer and we were very pleased with the stage performance. Absent the constraints of the 14 week lead time, and with a bit richer budget, we would probably have opted for an alumina ceramic base spar, and a carriage made from lightweighted silicon nitride, with an eye towards pushing the carriage-air bearing torsional resonance higher, and tuning for higher bandwidth. Additional investments in the vibration isolation system could further reduce the position tracking error. That said, the existing performance would clearly qualify as “none too shabby”.

The author gratefully acknowledges the assistance of Bill Letendre in modeling this system.